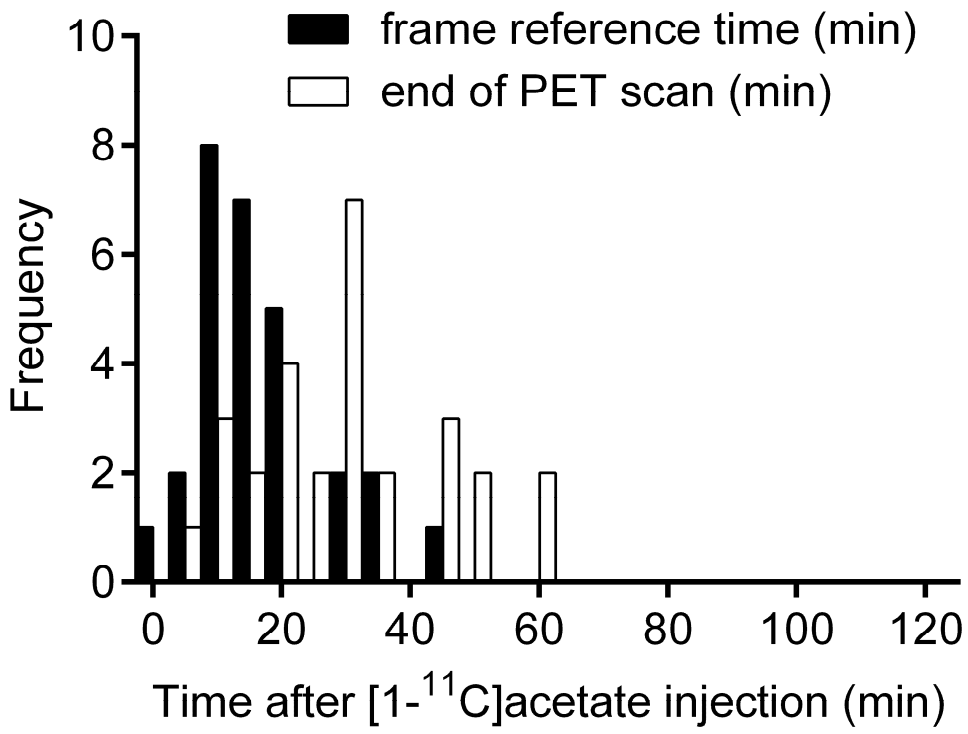

SUPPLEMENTAL FIGURE 1. Histogram showing the large variation in the timing of PET imaging protocols for [1-^{11}C]acetate in clinical oncology. The frame reference time is the midpoint of the time frame after [1-^{11}C]acetate injection that was used for analysis. In other words if the scan was acquired from 10 to 20 min after [1-^{11}C]acetate injection then the frame reference time was 15 min p.i. The data were taken from 28 separate studies (no data was available in 2 studies), details are given in Supplemental Table 1.

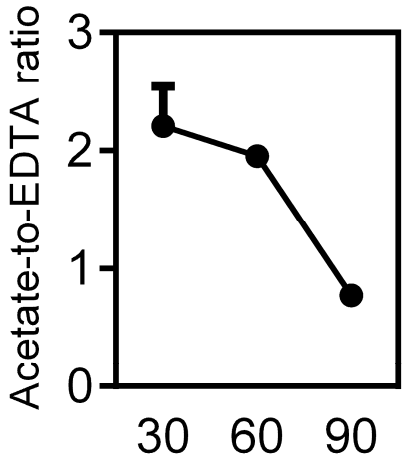

SUPPLEMENTAL FIGURE 2. ^{13}C NMR measurements of [1-^{13}C]acetate in aqueous tumor extracts of prostate-tumor bearing mice (bars represent mean + S.E.M (n = 1 – 2 mice at each time point)).

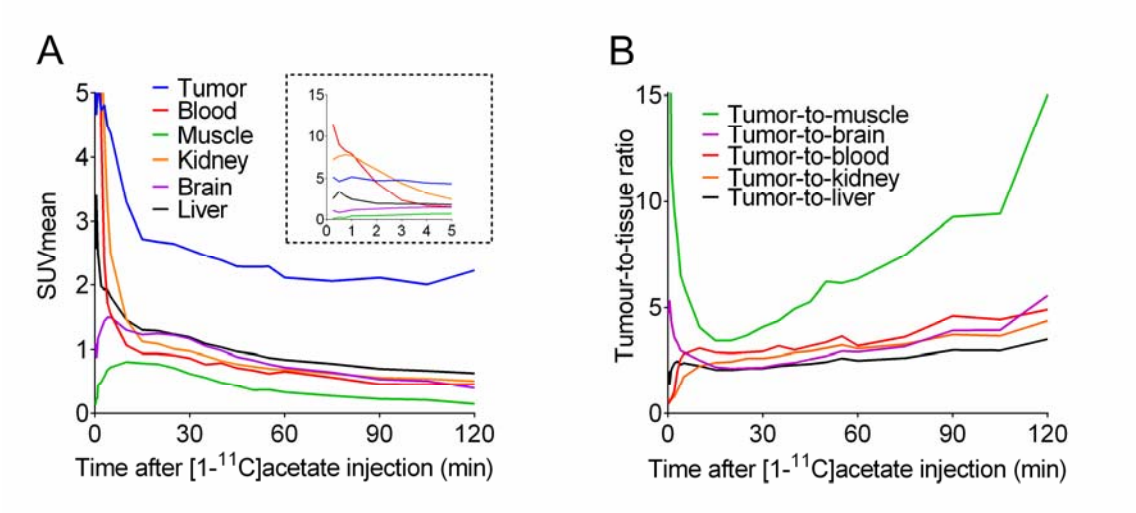

SUPPLEMENTAL FIGURE 3. Dynamic measurements of [1-^{11}C]acetate uptake in a K-ras^{G12D}; p53^{null} lung tumor-bearing mouse. (A) Tissue-time activity curves following [1-^{11}C]acetate injection from a single animal that was representative of others in the group (Figure 5 main article), *inset* shows the first 5 minutes. (B) Tumor-to-tissue activity ratios corresponding to the data shown in A.

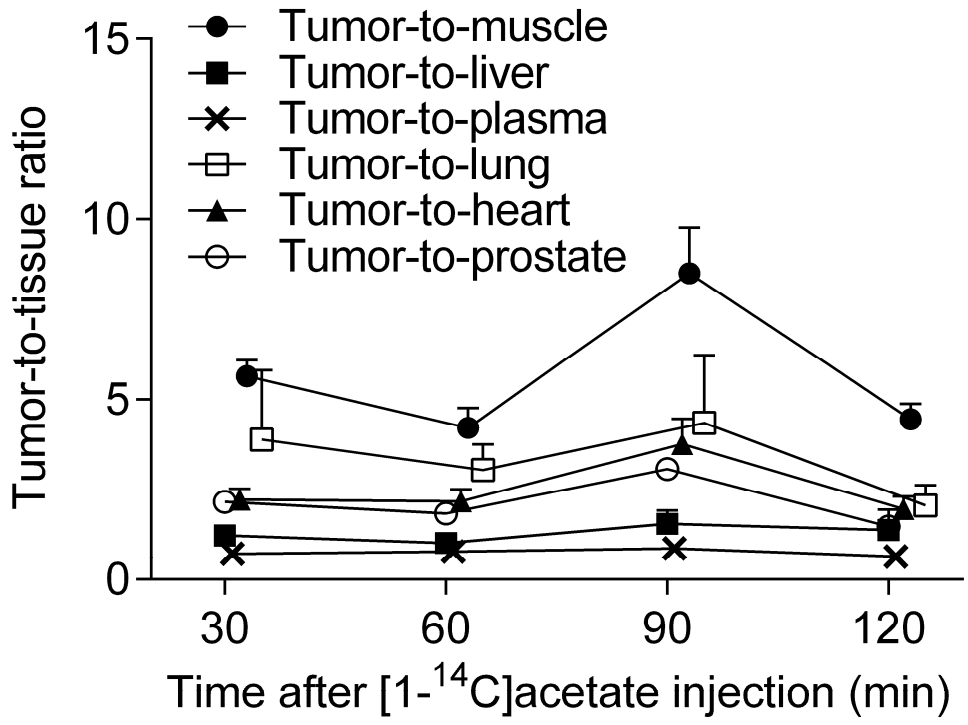

SUPPLEMENTAL FIGURE 4. Ratio between the ^{14}C content (%ID/g of tissue) in extracts of subcutaneous C4-2B prostate tumors versus extracts of other tissues at the specified times following i.v. injection of [1-^{14}C]acetate (points represent the mean ± S.E.M. for n = 8 or 9 at each time point).

SUPPLEMENTAL METHODS

^{13}C NMR spectroscopy in C4-2B xenografts

The aqueous fractions of tumor extracts were reconstituted in $^{2}H_2O$ containing 200 mmol/l phosphate buffer, pH 7, and 10 mmol/l EDTA. Extracts were prepared from tumors at 30 (n = 2), 60 (n = 1) and 90 min (n = 1) following administration of [1-^{13}C]acetate. Proton decoupled ^{13}C-NMR spectra were acquired using a Bruker Avance II+ 500 MHz spectrometer (Bruker Biospin, Karlsruhe, Germany), with a 30° flip angle pulse, Waltz-16 decoupling, a relaxation delay of 2 s and are the sum of 4096 transients. The integral of the [1-^{13}C]acetate resonance was normalized with respect to the integrals from the EDTA resonances and corrected for tumor weight.

^{13}C metabolite analysis by GC-MS in C4-2B xenografts

One µl of each derivatized sample was injected using an MP Multipurpose sampler MPS2-Twister (Gerstel, Germany) into an Agilent 7890A gas chromatograph (Agilent Technologies, US), separated on a Phase RXI-5Sil MS, 30m x 0.25mm (Restek, UK) GC column using helium (N6.0, Boc UK) as a carrier gas at constant flow rate of 1 ml/min.

GC Method for non-aqueous fraction samples

The injector temperature was heated to 270 °C. GC oven temperature was set at 100 °C for the first 5 minutes and then programmed to ramp up by 15 °C/min to 200 °C, 5 °C/min to 250 °C and finally 15 °C/min to 300 °C. Transfer line temperature was kept at 230 °C. Data collection rate was set to 20 Hz. Acquisition delay was 300 seconds.

GC Method for aqueous fraction samples

The injector temperature was held at 230 °C. GC oven temperature was set at 80 °C for the first 2 minutes and then programmed to ramp up by 15 °C/min to 300 °C, and then maintained at 300 °C for 6 minutes. Transfer line temperature was kept at 250 °C. Data collection rate was set to 20 Hz. Acquisition delay was 300 seconds.

MS method

A Pegasus High-Throughput (HT) Time of Flight (TOF) Mass Spectrometer (Leco, UK) was used to detect mass spectra of analytes. Eluted analytes from the GC column were introduced into electron impact ion source and ionized at 70 eV. Masses were scanned in the range of 85 to 500 Da. Acquisition rate was set at 20 spectra per second. Detector voltage was set at 1500 V and ion source temperature to 230 °C.

SUPPLEMENTAL TABLE

Supplemental Table 1. Published clinical [1-^{11}C]acetate PET studies showing the amount of radioactivity injected, the start time and duration of PET image acquisition following [1-^{11}C]acetate injection. Conditions of the PET scan are summarized, where available, in the following format: Time frame used for analysis of summed PET image in minutes; @ time frame acquisition interval in minutes after tracer injection ('p.i.); end of acquisition in minutes after injection in brackets; and mean injected activity in MBq. Abbreviations: T/N – tumor-to-normal tissue ratio; TAC – Time-Activity Curve; FOV – Field-of-View; BAC – bronchioalveolar carcinoma; WDA –well differentiated lung adenocarcinoma; HCC – hepatocellular carcinoma; RCC – renal cell carcinoma; and BPH – benign prostate hyperplasia.

Publication	Cancer	Conditions	Result	Comment
(*1*)	Prostate	10'@10-20'p.i. 740 MBq	SUV 3.3-10 all lesions detected	
(*2*)	Prostate	10'@47' p.i. 520 MBq	Radiotherapy patients Mean SUVmax 2.9, mean T/N 2.4, Surgery Patients: T/N 1.9. PSA <0.8 ng/ml	Old scanner (partial volume effects), count rate in saturation, no CT fusion).
(*3*)	Prostate	2'@10-12'p.i. (max 30') 1.5 GBq Dynamic acquisition 0 – 6'p.i., alternating bed positions thereafter	Acetate uptake in tumors was similar to that in benign prostatic hyperplastic nodules. Sensitivity and specificity of 61.6% and 80.0%, only Logan plot was linear.	Possibly imaging blood flow as the time frame 10 – 12'p.i. was used for analysis and the scan stopped at 30'.
(*4*)	Prostate	5'@5'p.i. (5'per bed position) 950 MBq	Failed to detected small nodule involvement	Not clear which was the first bed position and when the prostate was in the FOV
(*5*)	Prostate	20' @ 0-20' p.i. 5.5 MBq/kg Dynamic acquisition	3-compartment kinetic model was adequate. Early to late SUV comparison provided significant difference between primary and recurrent cancer but not BPH.	Possibly imaging blood flow.
(*6*)	Prostate	10 MBq/kg started at injection		Reference time frame and scan duration was not reported.

Publication	Cancer	Conditions	Result	Comment
(*7*)	Prostate	10'@2-12' (max 47') 524 MBq		Late time frames were acquired over regions other than prostate.
(*8*)	Prostate	4'@ 10-14' p.i. (max 34' p.i.) 642 MBq	Acetate uptake was visualized in all patients. No correlation between SUVmax and Gleason score.	Late time frames were acquired over regions other than prostate.
(*9*)	Prostate	4'@16'-20'p.i. (max 20' p.i.) 555 MBq dynamic acquisition 10x30" 15x60" time frames	Little difference between normal, BPH and cancer. No difference between early (6-10'p.i.) and late (16-20' p.i.) images.	Late images may not have been late enough.
(*10*)	Recurrent Prostate	First bed position 5'@5' p.i. 810 MBq		Number of bed positions was not indicated, nor was it clear which was the first bed position
(*11*)	Recurrent prostate	@10' p.i. 800 MBq	Promising results for recurrence detection with low PSA values	Scan duration is not reported. Not clear which was the first bed position and when the prostate was in the FOV
(*12*)	Bone metastatic prostate	20' @ 5 – 25' p.i. 11 MBq/kg	Acetate PET generally detected more metastases with a higher T/N ratio than FDG. Acetate could be used for tumor response assessment. T/N ratio was most useful.	Late time frames were used for qualitative metastases detection.
(*13*)	Lung	4.6 MBq/kg @ 10' p.i. up to 24'	Acetate sensitivity 71% (57% FDG), with the same specificity. For WDA sensitivity of acetate and FDG were 67% and 37% respectively	Could replace FDG for imaging of NSCLC

Publication	Cancer	Conditions	Result	Comment
(*14*)	Lung	3'@10'-34' p.i. (8 time frames) 4.6 MBq/kg	Image BAC and WDA with higher sensitivity than FDG, cannot evaluate aggressiveness as well as FDG. Acetate provides complementary to FDG information.	Not clear which was the first bed position and when the lung was in the FOV
(*15*)	Lung	10'@10-20' p.i. (max 26'p.i.) 555 MBq Dynamic acquisition	Acetate is inferior to FDG. SUVs ranging from 0.14 to 5.50.	Possibly imaging blood flow. Acetate provided complementary information to FDG
(*16*)	HCC	10'@10-20'p.i. (max 30'p.i.) 555 MBq Two bed positions used.	SUV [SUVmax] 7.32 , T/N 1.96	Not clear which time frame provided data for SUV calculations. Acetate provided complementary information to FDG
(*17*)	HCC	3'@20'-38' p.i. (max. 41' p.i.) 370-555 MBq	Acetate PET increased sensitivity of primary tumor detection compared to FDG PET, but not of metastases.	Not clear when the liver or extrahepatic metastases were in the FOV.
(*18*)	HCC	5'@15'-30' p.i. (max 45' p.i.) 850 MBq	87% sensitivity was reported. Acetate PET might play a role in HCC diagnostic workup.	Not clear when the prostate was in the FOV
(*19*)	Renal (clear cell and papillary carcinoma)	30'@ 20-50' p.i. 370 MBq 9x10" 7x30" 5x60" 2x300"	70% positive findings. Marked uptake in renal cell carcinoma that was dependent on tumor size. Acetate is a possible PET tracer for detection of renal cell carcinoma. (T/N 1.5 and 3)	At least 15' p.i. is recommended.
(*20*)	Renal (clear cell carcinoma and papillary)	25'@5-30'p.i. 840 MBq Dynamic acquisition: 12×10", 2×30", 2×60", 2×150", 4×300"	The majority of RCCs accumulated acetate to a lesser or similar extent compared with normal kidney parenchyma. T/N 2 and 4. Acetate PET cannot be recommended for the characterization of a renal mass.	Images analyzed on summed 5-30' time frames. Possibly wrong conclusions from the shape of TAC.

Publication	Cancer	Conditions	Result	Comment
(*21*)	Renal	Dynamic acquisition 10x10" 10x20" 2x2.5' 4x5' (max 30' p.i.) 370-740 MBq	acetate promising with kinetic modeling	Difference in tracer kinetics after 10'p.i. was reported for renal parenchyma and RCC
(*22*)	Renal oncocytoma and recurrent prostate	5'@10' p.i. 1460 MBq	Both tumor types detected.	Case report. Not clear when prostate was in the FOV nor what was the scan duration.
(*23*)	Renal	unknown	Acetate PET positive while FDG PET negative. Acetate PET predictive of response at 2 weeks.	TK inhibitor treatment response case report, no imaging details reported.
(*24*)	Bladder	3-5' @approx.15, 25' p.i. (max.60' p.i.) 760 MBq	Detection of residual bladder cancer sensitivity 80% specificity 50% Identification of metastatic nodal regions sensitivity 100% specificity 87%.	Not clear when the tumor was in FOV for SUV calculations. Intermediate phase thought to be best for imaging 15-20min p.i. but not a clear rationale given.
(*25*)	Head and Neck: squamous cell carcinoma	5'@17-22' (max 32'p.i.) 10 MBq/kg Dynamic acquisition.	Acetate detected more lesions than FDG. Acetate provided larger tumor volumes.	Thresholding with background correction was used to calculate SUVs.
(*26*)	Glioma	6 MBq/kg @ 5 – 15' p.i.	Acetate high sensitivity - 90%, uptake proportional to grade.	Compared to methionine which did not distinguish grade.
(*27*)	Glioma	740 MBq @ 10 – 20'p.i.	Acetate differentiated low and high grade lesions	FDG was not useful for grading
(*28*)	Astrocytoma	740 MBq @3' p.i. for 20'	Acetate useful in detection but not grading	

Publication	Cancer	Conditions	Result	Comment
(*29*)	Meningioma	740 MBq @10’ p.i. for 10’	Acetate good for detection and monitoring therapy but not grading. T/N 3.46 uptake was not proportional to grade	Spatial dissociation of acetate and FDG.
(*30*)	Multiple myeloma	555 MBq @20’ p.i.	Acetate and FDG uptake in the same lesions	

REFERENCES

1. Oyama N, Akino H, Kanamaru H, et al. ^{11}C-acetate PET imaging of prostate cancer. *J Nucl Med.* 2002;43:181-186.

2. Albrecht S, Buchegger F, Soloviev D, et al. ^{11}C-acetate PET in the early evaluation of prostate cancer recurrence. *Eur J Nucl Med Mol Imaging.* 2007;34:185-196.

3. Mena E, Turkbey B, Mani H, et al. ^{11}C-Acetate PET/CT in localized prostate cancer: a study with MRI and histopathologic correlation. *J Nucl Med.* 2012;53:538-545.

4. Kotzerke J, Volkmer BG, Glatting G, et al. Intraindividual comparison of [^{11}C]acetate and [^{11}C]choline PET for detection of metastases of prostate cancer. *Nuklearmedizin.* 2003;42:25-30.

5. Schiepers C, Hoh CK, Nuyts J, et al. 1-^{11}C-acetate kinetics of prostate cancer. *J Nucl Med.* 2008;49:206-215.

6. Fricke E, Machtens S, Hofmann M, et al. Positron emission tomography with ^{11}C-acetate and ^{18}F-FDG in prostate cancer patients. *Eur J Nucl Med Mol Imaging.* 2003;30:607-611.

7. Vees H, Buchegger F, Albrecht S, et al. ^{18}F-choline and/or ^{11}C-acetate positron emission tomography: detection of residual or progressive subclinical disease at very low prostate-specific antigen values (< 1 ng/mL) after radical prostatectomy. *BJU Int.* 2007;99:1415-1420.

8. Jambor I, Borra R, Kemppainen J, et al. Functional imaging of localized prostate cancer aggressiveness using ^{11}C-acetate PET/CT and ^{1}H-MR spectroscopy. *J Nucl Med.* 2010;51:1676-1683.

9. Kato T, Tsukamoto E, Kuge Y, et al. Accumulation of [^{11}C] acetate in normal prostate and benign prostatic hyperplasia: comparison with prostate cancer. *Eur J Nucl Med Mol Imaging.* 2002;29:1492-1495.

10. Kotzerke J, Volkmer BG, Neumaier B, Gschwend JE, Hautmann RE, Reske SN. Carbon-11 acetate positron emission tomography can detect local recurrence of prostate cancer. *Eur J Nucl Med Mol Imaging.* 2002;29:1380-1384.

11. Sandblom G, Sorensen J, Lundin N, Haggman M, Malmstrom PU. Positron emission tomography with C11-acetate for tumor detection and localization in patients with prostate-specific antigen relapse after radical prostatectomy. *Urology.* 2006;67:996-1000.

12. Yu EY, Muzi M, Hackenbracht JA, et al. C11-acetate and F-18 FDG PET for men with prostate cancer bone metastases: relative findings and response to therapy. *Clin Nucl Med.* 2011;36:192-198.

13. Nomori H, Shibata H, Uno K, et al. ^{11}C-acetate can be used in place of ^{18}F-fluorodeoxyglucose for positron emission tomography imaging of non-small cell lung cancer

with higher sensitivity for well-differentiated adenocarcinoma. *J Thorac Oncol.* 2008;3:1427-1432.

14. Shibata H, Nomori H, Uno K, et al. ^{11}C-acetate for positron emission tomography imaging of clinical stage IA lung adenocarcinoma: comparison with ^{18}F-fluorodeoxyglucose for imaging and evaluation of tumor aggressiveness. *Ann Nucl Med.* 2009;23:609-616.

15. Higashi K, Ueda Y, Matsunari I, et al. ^{11}C-acetate PET imaging of lung cancer: comparison with ^{18}F-FDG PET and ^{99m}Tc-MIBI SPET. *Eur J Nucl Med Mol Imaging.* 2004;31:13-21.

16. Ho CL, Yu SC, Yeung DW. ^{11}C-acetate PET imaging in hepatocellular carcinoma and other liver masses. *J Nucl Med.* 2003;44:213-221.

17. Park JW, Kim JH, Kim SK, et al. A prospective evaluation of ^{18}F-FDG and ^{11}C-acetate PET/CT for detection of primary and metastatic hepatocellular carcinoma. *J Nucl Med.* 2008;49:1912-1921.

18. Li S, Beheshti M, Peck-Radosavljevic M, et al. Comparison of ^{11}C-acetate positron emission tomography and ^{67}Gallium citrate scintigraphy in patients with hepatocellular carcinoma. *Liver Int.* 2006;26:920-927.

19. Oyama N, Okazawa H, Kusukawa N, et al. ^{11}C-acetate PET imaging for renal cell carcinoma. *Eur J Nucl Med Mol Imaging.* 2009;36:422-427.

20. Kotzerke J, Linne C, Meinhardt M, et al. [1-^{11}C]acetate uptake is not increased in renal cell carcinoma. *Eur J Nucl Med Mol Imaging.* 2007;34:884-888.

21. Shreve P, Chiao PC, Humes HD, Schwaiger M, Gross MD. Carbon-11-acetate PET imaging in renal disease. *J Nucl Med.* 1995;36:1595-1601.

22. Shriki J, Murthy V, Brown J. Renal oncocytoma on 1-^{11}C acetate positron emission tomography: case report and literature review. *Mol Imaging Biol.* 2006;8:208-211.

23. Maleddu A, Pantaleo MA, Castellucci P, et al. ^{11}C-acetate PET for early prediction of sunitinib response in metastatic renal cell carcinoma. *Tumori.* 2009;95:382-384.

24. Schoder H, Ong SC, Reuter VE, et al. Initial results with ^{11}C-acetate positron emission tomography/computed tomography (PET/CT) in the staging of urinary bladder cancer. *Mol Imaging Biol.* 2012;14:245-251.

25. Sun A, Sorensen J, Karlsson M, et al. 1-[^{11}C]-acetate PET imaging in head and neck cancer - a comparison with ^{18}F-FDG-PET: implications for staging and radiotherapy planning. *Eur J Nucl Med Mol Imaging.* 2007;34:651-657.

26. Yamamoto Y, Nishiyama Y, Kimura N, et al. ^{11}C-acetate PET in the evaluation of brain glioma: comparison with ^{11}C-methionine and ^{18}F-FDG-PET. *Mol Imaging Biol.* 2008;10:281-287.

27. Tsuchida T, Takeuchi H, Okazawa H, Tsujikawa T, Fujibayashi Y. Grading of brain glioma with 1-^{11}C-acetate PET: comparison with ^{18}F-FDG PET. *Nucl Med Biol.* 2008;35:171-176.

28. Liu RS, Chang CP, Chu LS, et al. PET imaging of brain astrocytoma with 1-^{11}C-acetate. *Eur J Nucl Med Mol Imaging.* 2006;33:420-427.

29. Liu RS, Chang CP, Guo WY, et al. 1-^{11}C-acetate versus ^{18}F-FDG PET in detection of meningioma and monitoring the effect of gamma-knife radiosurgery. *J Nucl Med.* 2010;51:883-891.

30. Lee SM, Kim TS, Lee JW, et al. Incidental finding of an ^{11}C-acetate PET-positive multiple myeloma. *Ann Nucl Med.* 2010;24:41-44.